NURETH14-212

Experimental study on the pool boiling CHF enhancement using magnetic fluid

Jong Hyuk Lee[1] and Yong Hoon Jeong[1,2]
[1]Dept. Of Nuclear and Quantum Eng. Korea Advanced Institute of Science and Technology,
373-1, Guseong-dong, Yuseong-gu, Daejeon 305-701, Republic of Korea
leejonghyuk@kaist.ac.kr, jeongyh@kaist.ac.kr

[2]Department of Nuclear Engineering, Khalifa University of Science, Technology & Research (KUSTAR)
P.O.Box 127788, Abu Dhabi, UAE

Abstract

This paper will describe the effects of magnetic fluid on CHF enhancement of pool boiling. In order to evaluate the effects as nanoparticle characteristic of magnetic fluid, we compared the CHF values of pool boiling experiment between magnetic fluid and other nanofluids with several volume concentrations. SEM(Scanning Electron Microscope) images were obtained to explain CHF enhancement through the effect of the deposited nanoparticles, which can change the surface wettability, during the pool boiling experiment. Lastly, the analysis for bubble formation in pool boiling using image processing was performed to demonstrate between the characteristics of bubble formation and CHF enhancement.

1. Introduction

One of the key research areas in the cooling systems of nuclear reactors, nuclear fusion reactors, thermal power plants, and others is the removal of high heat flux to guarantee the efficiency, performance, and safety. In the process of removing high heat flux, nucleate boiling is a very effective heat transfer mechanism. However, it is well known that there exists a critical value of heat flux at which nucleate boiling transitions to film boiling shows very poor heat transfer behavior. Critical heat flux(CHF) is a main constraint to the design process because it can generate damages or deformations of material. But, the mechanisms and prediction methods of CHF occurrence are not revealed exactly. Therefore, there have been many efforts to clarify the mechanism of CHF occurrence and also to improve the CHF using nanofluids by researchers [1-5]. The results of existing studies can be summarized as follows:

· Significant CHF enhancement (up to 200%) occurs with various nanoparticle materials, including silicon, aluminum and titanium oxides.

· The CHF enhancement occurs at relatively low nanoparticle concentrations, typically less than 1% by volume.

· During nucleate boiling, nanoparticles are deposited on the heater and formed a thin layer which depends on each kind of nanoparticle.

· It is difficult to disperse nanoparticles and maintain the dispersed condition of nanoparticles. Therefore, there are difficulties in the repeatability of experiments.

In this study, a magnetite-water nanofluid (MWNF) is introduced to overcome the shortcomings of nanofluids. MWNF is a colloidal suspension consisting of magnetic nanoparticles and carrier liquid. The chemical, mechanical and other physical properties of MWNF correspond very closely to those of the carrier liquid [6]. MWNF behaves as not only the flow features like the conventional nanofluid, but also the magnetic features similar to flowability of the bulk magnetic materials. Therefore, MWNF is strongly affected by an applied magnetic field. In a uniform magnetic fluid, the particles in a magnetic fluid align with the field. In a gradient field, however, the particles experience a force such that the fluid itself responds as a homogenous magnetic liquid which moves to the region of the highest field. Thus, MWNF can be precisely positioned and controlled by an external magnetic field. However, there have been few detailed studies on the pool boiling CHF enhancement using these characteristics of magnetic fluid. Thus, the present study aims at investigating pool boiling CHF enhancement using MWNF.

This paper will describe the characteristics of MWNF on CHF enhancement of pool boiling. In order to compare the degree of CHF enhancement between MWNF and other nanofluids, the pool boiling experiments were performed with volume concentrations from 10^{-4} to 10^{-2} %. Scanning electron microscope (SEM) images were obtained to explain CHF enhancement through the effect of the deposited nanoparticles, which can change the surface wettability, during the pool boiling experiment.

2. Experiment

2.1 Preparation and characteristics of nanofluids

Three kinds of nanofluids were prepared for pool boiling experiments using magnetite, alumina and titania nanoparticles which were manufactured by Nanostructured & Amorphous Material Inc. (NanoAmor) and, Table I shows the properties of them. A two-step method was used to produce nanofluids with each volume concentrations of nanoparticles. The first stage is to mix nanoparticles with a nominal particle size of 30±5nm in Distilled water. The next stage is to homogenize the mixture using ultrasonic vibration at sound frequencies of 40 kHz. Since the ultrasonic vessel causes the nanoparticles in the mixture to vibrate, it breaks down agglomerates.

Table I. Properties of Nanoparticles

Nanoparticles	Fe_3O_4	Al_2O_3	TiO_2
Density (g/cc)	5.10	3.96	3.78
Specific surface area(m^2/g)	66	180	240
Averaged particles size(nm)	25	40-80	15
Particle Morphology	Spherical	Spherical	Spherical

$$\phi_v = \frac{1}{\left(\frac{1-\phi_m}{\phi_m}\right)\frac{\rho_p}{\rho_f}+1} \qquad (1)$$

In this study, all concentrations of nanofluids were considered by volume fraction ϕ_v. Because the flow phenomenon of a liquid-solid fluid depends on the hydrodynamics force acting on the surface of solid particles. Because of difficulties involved in precisely measuring volume of nanoparticle, the following conversion formula (Eq. 1) is conventionally used, where ϕ_m is the mass concentration of nanoparticles, ρ_p is the nanoparticle density and ρ_f is the fluid density.

Before applying nanofluids to CHF experiments, a precondition is to keep a uniform dispersion and stable suspension of nanoparticles in the liquids. Because of agglomerated nanoparticles, the characteristics of nanofluids can be changed. Zeta potential is well known as standards for the stable level of nanofluids. Thus, magnetite nanoparticles having the highest density among prepared nanoparticles are chosen to measure the zeta potential.

Generally, a zeta potential above 30 mV reflects physically stablility, while a suspension with a zeta potential below 20 mV has limited stability. A suspension with a zeta potential below 5 mV undergoes pronounced aggregation. In this study, zeta potential was measured using a Zeta-plus by Brookhaven Instruments Ltd. 100ppm MWNF was made by using ultrasonic vessel over 3 hours. After the nanofluids were preserved for 1h, 12h and 24h, respectively, zeta potential was measured. Figure 1 shows the measured zeta potential of 100ppm MWNF as a function of preserved time. The values were over 30mV, although the zeta potential decreased according to the preserved time. The results verify 100ppm MWNF will be preserved in a stable condition for 24 hours.

$$q''_{CHF} = \frac{V_{max} \times I_{max}}{\pi D L} \qquad (2)$$

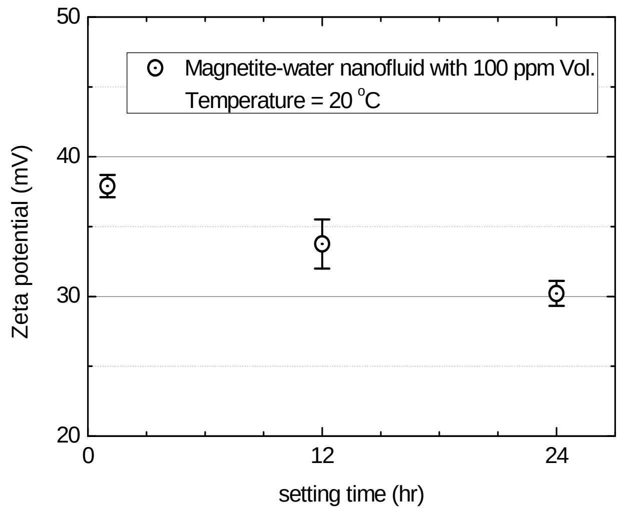

Figure 1 Zeta potential results of Fe_3O_4 nanoparticles in distilled water according to the changes of setting time.

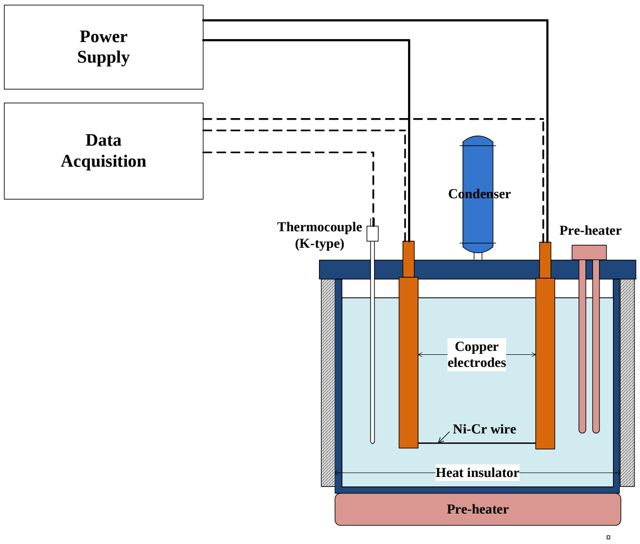

Figure 2 Schematic of the pool boiling apparatus

2.2 Experiment apparatus and procedures

Figure 2 shows a schematic of the experimental apparatus. The pool boiling experimental system consists of a 250 X 100 X 230 mm rectangular main vessel which is made of stainless steel with visualization windows, a pre-heater, copper electrodes, a thermocouple(K-type) to measure pool temperature, and a condenser. The condenser maintains atmospheric pressure inside the chamber and prevents the loss of vapor from the vessel. A Ni-Cr wire, as a heater, with a diameter of 0.4mm was used as boiling surface and was heated by the DC power supply of OPE-3050DI with a maximum capacity of 1.5kW(50V, 30A). The signals of voltage, current and temperature were measured with a National Instrument data acquisition system.

All pool boiling experiments were performed after the bulk temperature of the working fluid was kept at the saturated temperature (100°C). The experiment was performed by gradually increasing the electric power supplied to the wire with a regular pattern. The power was initially increased in large steps and then, near the expected CHF value, the power was increased in small steps. When the expected CHF value was reaches, the resistance of the Ni-Cr wire sharply increased and the wire became red-hot or broke suddenly. The CHF was calculated by Eq.(2) using data obtained right before sharp increase of Ni-Cr wire resistance.

3. Experimental results

Two sets of experiment results were obtained. First, pool boiling CHF experiment included for the results of pool boiling CHF experiments using from 10^{-4} to 10^{-2} % of volume concentration of nanofluids. Second, CHF enhancement was investigated through SEM images, an analysis of bubble formation using image processing, and the effect of magnetic field in order to clarify the mechanisms of CHF enhancement.

3.1 Pool boiling CHF experiment

In order to investigate the characteristic of pool boiling CHF enhancement using nanofluid, the pool boiling experiments were performed with distilled water as the reference case in advance. The pool boiling CHF experiments with distilled water were conducted over 10 times to validate the repetition of experiment results. Measured CHF average value of distilled water was about 3% of the value predicted using Eq. (3) of Zuber[7]'s correlation, which has been widely used to predict pool boiling CHF.

$$q''_{CHF} = \frac{\pi}{24}\rho_g^{1/4} h_{fg} \sqrt[4]{g\sigma(\rho_f - \rho_g)} \tag{3}$$

where q" is heat flux, ρ_g, ρ_f the gas density and fluid density, respectively, h_{fg} denotes the latent heat of vaporization, g is gravity, and σ is surface tension.

Pool boiling CHF experiments were conducted with low volume concentrations from 1ppm to 3ppm of MWNF to check the feasibility of CHF enhancement using MWNF similar to other conventional nanofluids. The CHF results for MWNF with low concentrations are presented in Figure 3. According to the results, the CHF increases even at low concentrations from about 160% to 190% relative to CHF with the use of distilled water. Based on the results, the pool boiling CHF experiments with MWNF from 1 to 100ppm were also conducted. In order to compare the degree of CHF enhancement with MWNF, the pool boiling experiments with alumina water nanofluid (AWNF) and titania-water nanofluid (TWNF) were performed. Measured CHF data are shown in Figure 4. Figure 5 shows CHF values in nanofluids normalized by CHF of distilled water. Significant CHF enhancement is observed with all fluids but slight differences in CHF enhancement are due to the characteristics of the nanoparticles. CHF enhancement with MWNF was the highest in the range of 1 to 100ppm nanoparticle concentrations among the selected nanofluids in this study.

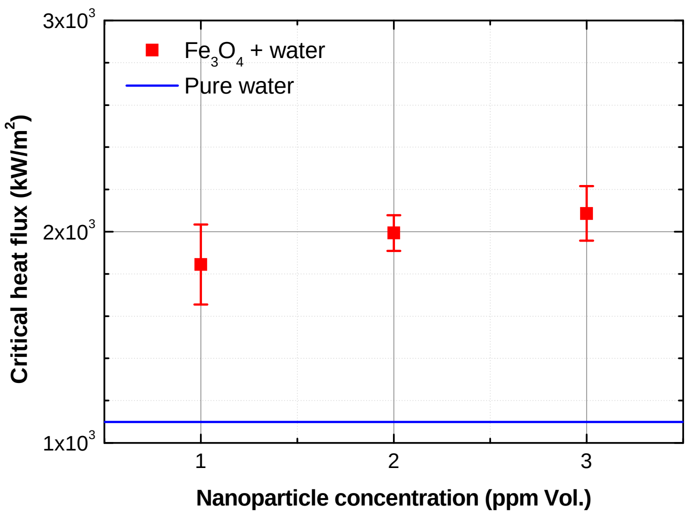

Figure 3 CHF data of magnetite-water nanofluid with from 1 to 3ppm nanoparticle concentration

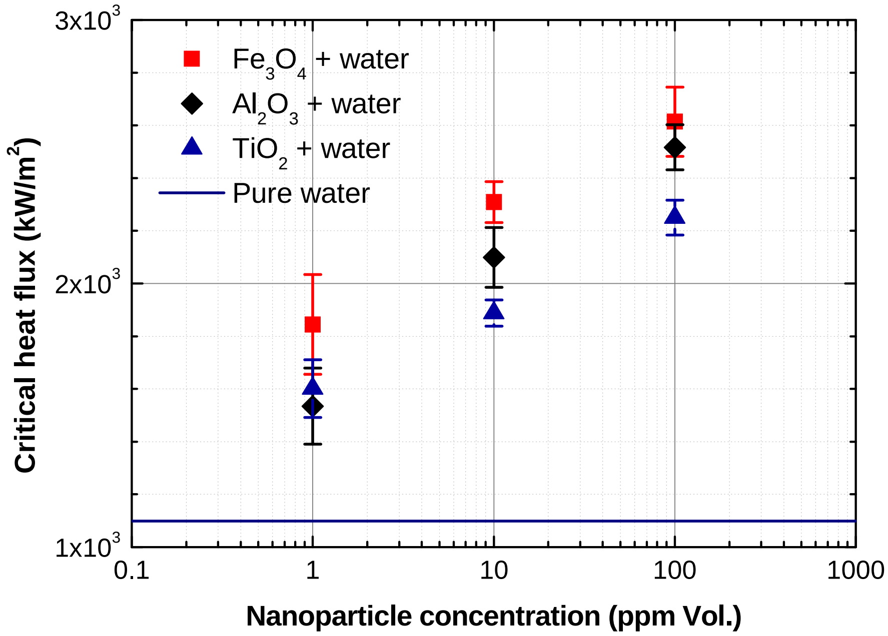

Figure 4 Comparison of CHF data between magnetite-water nanofluid and other water-based nanofluids

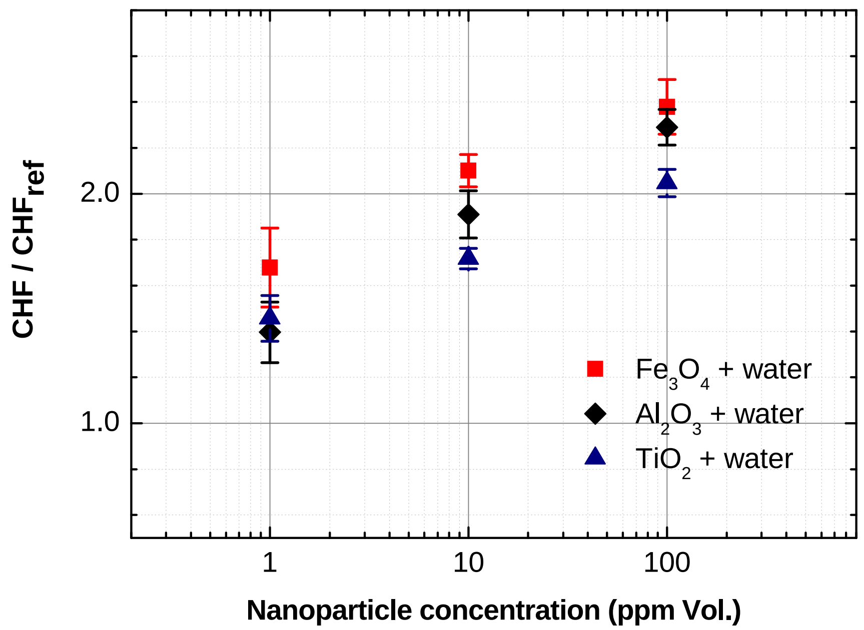

Figure 5 CHF ratio of nanofluids with from 1 to 100ppm nanoparticle concentrations

3.2 CHF enhancement

3.2.1 Effect of nanoparticle deposition

SEM images were acquired to explain the effect of nanoparticle deposition on CHF enhancement in nanofluid. Figure 6 shows SEM images of Ni-Cr wire surfaces after the pool boiling CHF experiments with MWNF and AWNF. Considerable amounts of nanoparticles were deposited on the Ni-Cr wire. The heated surfaces were changed by the deposition of nanoparticles. With higher the nanoparticle concentration, a larger amount of nanoparticles was deposited on the Ni-Cr wire. The deposited nanoparticles generated to porous layer on the Ni-Cr wire and the porous layer can be improved the wettability. In other words, it is easy to rewet the hot spots and cool the heated surface. This rewetting capability makes CHF of nanofluids enhanced. And, the degree of CHF enhancement was increased as the amount of deposited nanoparticles was increased. Therefore, CHF was more enhanced at high nanoparticles concentrations.

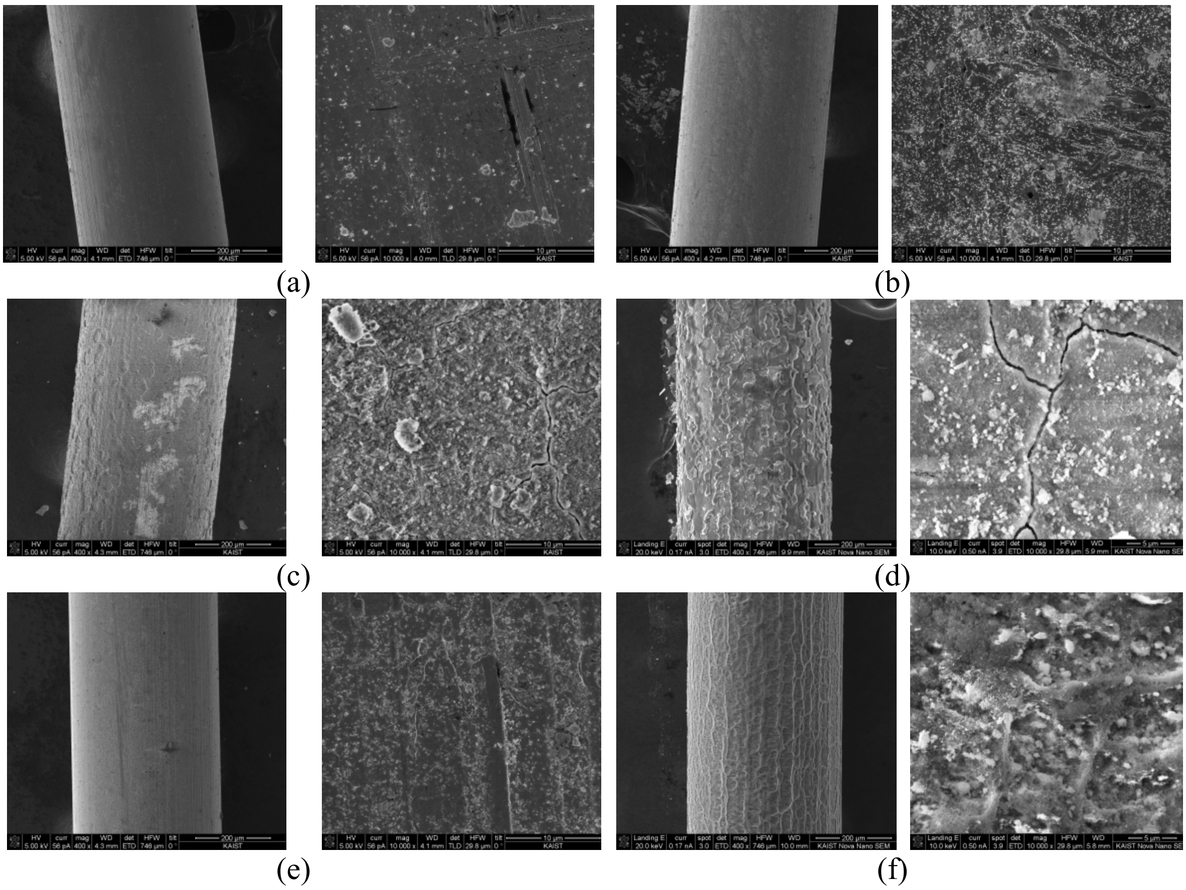

(a) (b) (c) (d) (e) (f)

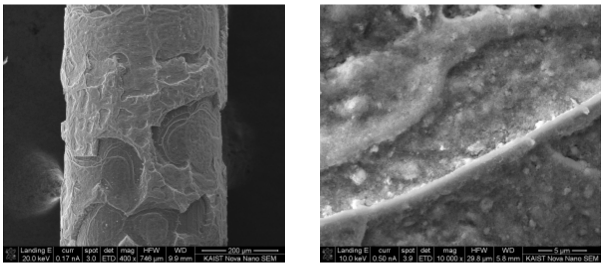

(g)

Figure 6 SEM images of wire surface after pool boiling (a) Distilled water (b) 1ppm of AWNF (c) 10ppm of AWNF (d) 100ppm of AWNF (e) 1ppm of MWNF (f) 10ppm of MWNF (g) 100ppm of MWNF (left x400, right x10000)

3.2.2 Effect of bubble formation in nucleate boiling

To understand the mechanism of CHF enhancement using MWNF, we focused on the bubble formation in the range of low heat flux of the heated surface, as a second method. The features of bubble formation like a frequency and diameter were analyzed by means of high-speed camera recording (2500 frames per second). In this study, the bubble frequency was obtained by observation and by calculation. To calculate the bubble frequency from the pictures, image processing using the algorithm of fast Fourier transform (FFT) was conducted. In advance, analysis of bubble frequency for pure water in nucleate boiling was conducted to validate the image processing code.

Figure 7(a) shows the results for pure water observed with an interval of 0.004s, when heat was supplied with 50kW/m^2. By using this images, we can get the frequency easily by observation. On the other hand, the pictures were converted to Figure 7(b) and the data were analyzed to acquire the results by using the FFT of MATLAB. The results by observation were compared with the ones by calculation in Table 2. The results were very similar within 7% error. Based on these results, we can conclude that the calculated results were reasonable to analyze the bubble frequency.

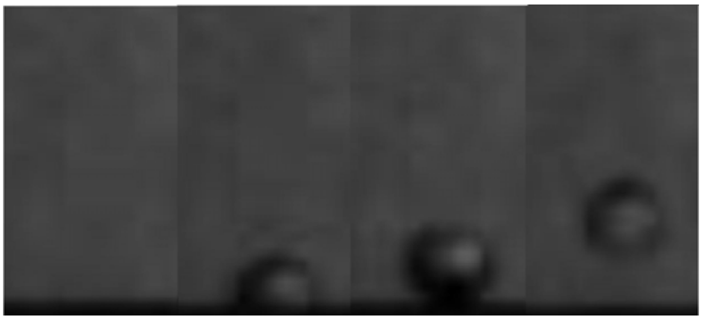

t = 0s   t = 0.004s   t = 0.008s   t = 0.012s

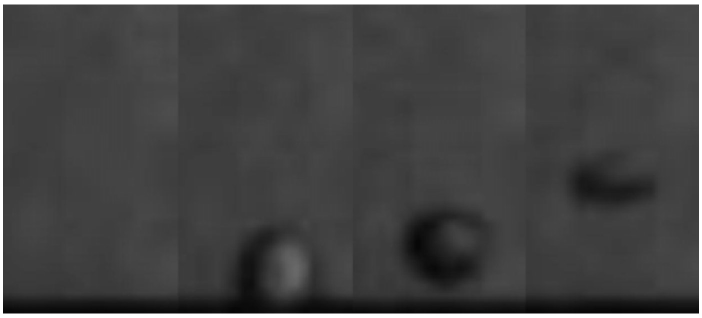

t = 0.032s   t = 0.036s   t = 0.040s   t = 0.044s

(a) By observation

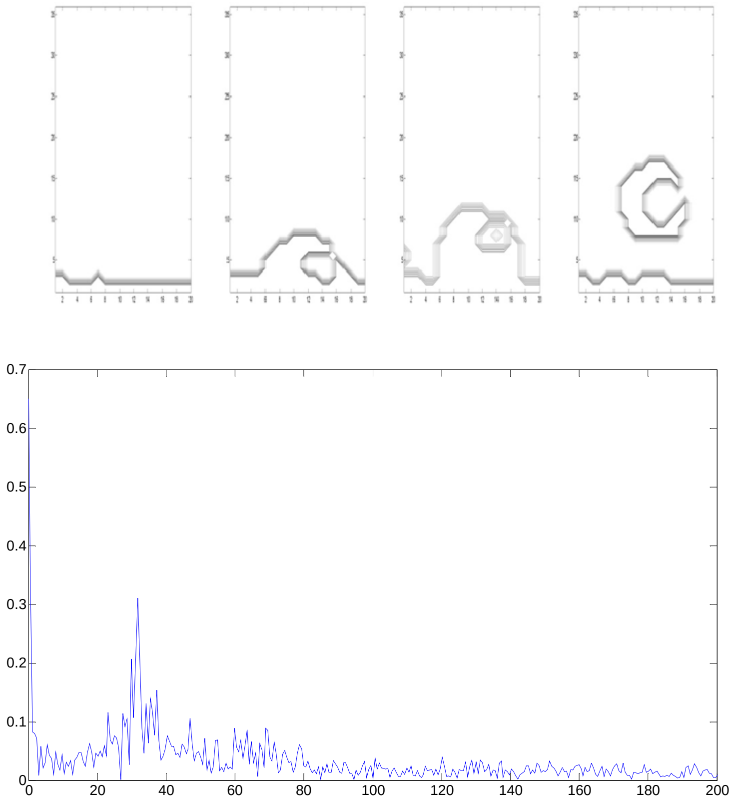

(b) By calculation

Figure 7 Comparison of bubble frequency between by observation and by calculation

By using this code, we also performed an analysis for 1ppm MWNF to compare the frequency between pure water and MWNF. The results are showed in Table 3. For pure water, the bubble frequency was within 20-35Hz when heat supply of 50kW/m^2. The averaged frequency using MWNF had about 2 times higher than the one of pure water at the same heat flux. And, it was difficult to find significant differences of bubble size between pure water and MWNF (figure 8). It means that the chance to rewet the same heated area in MWNF was relatively increased for the same time. Bubble frequency was determined by t_b (break-off time) and t_d (delayed time of bubbles). In other words, a bubble grows and remains with attaching to the heating surface during t_b until break-off from the heating surface. Following the departure of a bubble, liquid comes in contact with the heating surface and gets heated during a t_d at the end of which time another bubble is nucleated from the same position. This new bubble grows until t_b, it departs from the surface and the process is repeated. Both t_b and t_d for pure water and MWNF cases are plotted in figure 9. And also, figure 9 represents the fluid phase between a vapor and a liquid state on the heated surface. The time kept with vapor phase indicated that bubble remained on the heated surface until bubble departure, i.e., t_b. On the contrary, the time kept with liquid phase meant t_d for a period. From the results, t_b for MWNF case was shorter than the one for pure water case.

Table 2 Comparison of bubble frequency for several bubbles located on the wire

	Pure water	
	Observation	FFT
a	31	30~35
b	28	20~25
c	27	25~30
d	22	30~35

(unit : Hz)

Table 3 Comparison of bubble frequency between pure water and 1ppm of MWNF

	Pure water	MWNF
a	30~35	50~55
b	20~25	75~80
c	25~30	70~75
d	30~35	45~55

(unit : Hz)

(a)

(b)

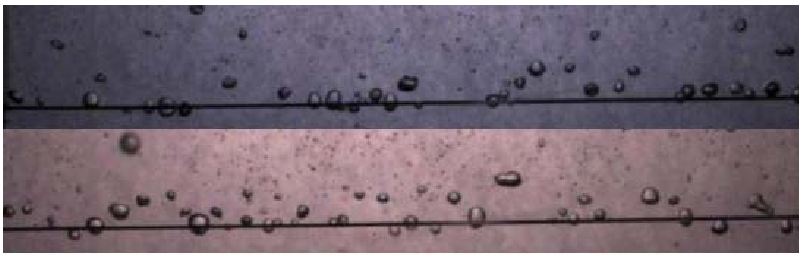

Figure 8 Photographs of pool boiling of (a) pure water; (b) 1ppm of the magnetite-water nanofluid with heat flux of 50kW/m^{-2}

We can conclude that the bubble formation in MWNF had higher frequency and the smaller bubbles, but with similar diameter, were formed. And t_b was shorter than t_d for a period. It means that heat, which is generated from Ni-Cr wire in MWNF, can be removed more frequently than the one in pure water, due to departed bubbles with short period. In addition to higher bubble frequency of MWNF, the time for bubble growth and departure is short. In other word, the heated surface in MWNF was rapidly and frequently rewetted. It means that surface wettability on the surface was improved and the onset of CHF can be delayed. Therefore CHF enhancement using MWNF can be explained by the improved surface wettability.

3.2.3 Effect of magnetic field

Based on pool boiling CHF experiment results according to the changes of nanofluid concentrations, the degree of CHF enhancement with MWNF was the highest among all applied nanofluids in all ranges of nanofluid concentration. Especially, it was remarkable that CHF enhancement with MWNF in the lower range of nanoparticle concentration was so high compared to the CHF enhancement of other nanofluids. In order to investigate the reason of CHF enhancement, we want to discuss the effect of magnetic field is considered.

A Heat flux in the pool boiling CHF experiments was controlled by an inputted voltage of power supply. When electric current is supplied through copper electrodes, magnetic field was induced by electric currents around Ni-Cr wire. In order to estimate the effect of magnetic field generated by electric currents, the Biot-Savart law was used to compute the magnetic field around Ni-Cr wire of pool boiling CHF experiment. The Biot-Savart law shows in Eq (4) having a derivative form.

$$d\vec{B} = \frac{\mu_0}{4\pi} I \frac{1}{r^2} d\vec{l} \times \vec{r} \tag{4}$$

Where dB is the contribution to magnetic field at a point r due to a segment dl of current I. μ_0 is permeability constant which is the measure of the ability of a material to support the formation of magnetic field in a vacuum. In other words, it is the degree of magnetization that a material obtains in response to an applied magnetic field. For a pool boiling CHF experiment with Ni-Cr wire, it was assumed that wire was infinitely long to calculate analytically magnetic field around Ni-Cr wire. Eq. (5) was used to calculate the magnetic field around Ni-Cr wire

$$B = \frac{\mu_0}{2\pi r} \bullet I \tag{5}$$

Here r is the distance perpendicular to the wire B is in the tangential direction and, I is electric currents across the wire.

Figure 9 shows analytic solutions, which were calculated by Eq. (5), for magnetic field around Ni-Cr wire according to the distance from the center of Ni-Cr wire. Applied currents in Eq. (5) were 16 and 17.5A, because the values were represented in the moment for occurring CHF with lower concentration of MWNF. From the results, magnetic flux intensity had the maximum values on the surface of Ni-Cr wire. Those values were around 160G ~180G (or 0.16~0.18T) of magnetic flux intensity. And, magnetic flux intensity was inversely proportional to the distance from the Ni-Cr wire in the radial direction. It is required to have little influence of the magnetic field over 0.1m distance from the center of Ni-Cr wire.

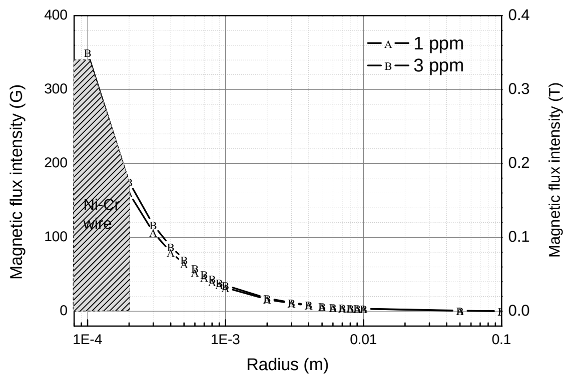

Figure 9. Analytic calculation results of magnetic field around Ni-Cr wire for 1-3ppm magnetite-water nanofluids cases.

As mentioned above, magnetic field is existed around Ni-Cr wire. Magnetite nanoparticles distribution in MWNF can be effectively controlled by applying a magnetic field [6]. As the distance from the wire is decreased, the magnetic field intensity becomes stronger. Because of stronger magnetic field near the wire, magnetite nanoparticles in MWNF congregated around the wire. Therefore, it is expected that the magnetite nanoparticles can be deposited on the wire more than other nanoparticles. And the local concentration or bubble kinetics can be changed by gathering magnetite nanoparticles around the wire. Thus, the degree of CHF enhancement can be also increased due to these effects of magnetic field. CHF enhancement compared to other nanofluids was remarkable in the range of lower concentration of MWNF. It is also expected that the effect of magnetic field can be more sensitive in lower nanoparticle concentration, relatively. As a further work, we should explain this hypothesis. To validate the hypothesis, the experimental study on characteristics of magnetic field in MWNF will be required.

4. Conclusions

The main findings of this study are as follows:

(1) Nanofluids with low concentration of alumina, titania and magnetite nanoparticles can significantly enhance the pool boiling CHF.
(2) After pool boiling experiments, considerable amount of nanoparticles were deposited on the wire. Because of this, surface wettability and surface tension, which are related to the important parameter CHF enhancement, are changed.
(3) Bubble frequency in magnetite-water nanofluid was higher than the one in pure water. Due to the emitted bubbles with higher frequency, surface wettability on the heater in magnetite-water nanofluid was enhanced.
(4) It is expected that CHF enhancement with low concentration of MWNF is affected by the effect of magnetic field which was induced by the electrical currents.

5. References

[1] S.M. You, J.H. Kim, K.H. Kim, Effect of Nanoparticles on Critical Heat Flux of Water in Pool Boiling Heat Transfer, Appl. phys. Lett. 83, 2003, pp. 3374.

[2] P. Vassallo, R. Kumar, S. D'Amico, Pool Boiling Heat Transfer Experiments in Silica-Water Nanofluids, Int. J. of Mass Transfer 47, 2004, pp. 407.

[3] I. C. Bang, S. H. Boiling Heat Transfer Performance And Phenomena of Al_2O_3-Water Nanofluids from a Plain Surface in a Pool, Int. J. Heat Mass Transfer 48, 2005, pp. 2407.

[4] H. Kim, M. Kim, Experimental Study of The Characteristics and Mechanism of Pool Boiling CHF Enhancement Using Nanofluids, Int. J. Heat Mass Transfer 45, 2009, pp. 991.

[5] S. Das, N. Puttra, W. Roetzel, Pool Boiling Heat Characteristics of Nanofluids, Int. J. Heat Mass Transfer 46, 2003, pp.851-862.

[6] K. Raj. And R. J. Boulton, "Ferrofluids – Properties and Applications," Material & Design, Vol. 8, No. 4, 1987, pp233.

[7] N. Zuber, Hydrodynamic Aspects of Boiling Heat Transfer, AEC Rep. AECU-4439,1959.